

Superfluid transition temperature of bond bipolarons with Coulomb interaction

Chao Zhang^{1,*}

¹*Department of Physics, Anhui Normal University, Wuhu, Anhui 241000, China*

Utilizing an exactly sign-problem-free quantum Monte Carlo method, we explore the influence of long-range Coulomb interaction on the superfluid transition temperature of bipolarons in two dimensions. The model studied here is the bond Su-Schrieffer-Heeger model with phonon-modulated electron hopping. Previously, in the absence of long-range Coulomb interaction, this model demonstrated the emergence of small-size, light-mass bipolarons that undergo a superfluid transition at high values of the transition temperature T_c [Physical Review X 13, 011010, (2023)]. Our findings indicate that even with the inclusion of long-range Coulomb interaction, T_c remains substantially high, even in the deep adiabatic regime where the phonon frequency is $\omega/t = 0.5$ and the Coulomb interaction $V = U/10$. This result suggests a physical mechanism for superconductivity in the low-density regime, which could hold relevance for ongoing experiments on dilute superconductors.

I. INTRODUCTION

Electron-phonon coupling is a fundamental interaction within condensed matter physics, giving rise to a variety of intriguing phenomena. This coupling reflects the intricate relationship between the dynamic behavior of electrons, which are the charge carriers, and the vibrational modes of the crystal lattice, known as phonons. The consequences of this interaction lead to significant modifications in electronic properties, such as the formation of polaron and bipolaron¹⁻⁷, changes in the effective mass of charge carriers⁸⁻¹⁰, and variations in charge carrier mobility and scattering¹¹. The polaron, formed through electron-phonon coupling, is particularly significant due to its connection to the mechanism of high-temperature superconductivity in the dilute-density regime. Under low-density conditions, electron-phonon interactions can pair two electrons into a single bipolaron, akin to the formation of a Bose-Einstein condensate-like superconductor. For such a superconducting state to occur, specific conditions must be met, including the presence of a bipolaron with a light effective mass, compact size, and a strong phonon-mediated pairing potential^{12,13}.

Depending on whether the phonon vibrations are coupled to the electron density or the hopping motion of the electron, two primary types of electron-phonon coupling exist: the Holstein and bond Su-Schrieffer-Heeger (SSH) models. Extensive prior research has revealed that in the Holstein model, where the electron-phonon coupling predominantly influences the electron density, the effective mass of both polaron and bipolaron grows exponentially at higher electron-phonon coupling strengths^{9,10,14,15}. In stark contrast, the scenario changes significantly when considering the bond SSH model, where the electron-phonon coupling perturbs the hopping of electrons. Recent investigations into bond SSH polarons have garnered substantial interest, chiefly due to the remarkable characteristic of a relatively light effective mass even in strong coupling regimes, resulting in a lightweight polaron¹⁵⁻¹⁷. Moreover, the bond SSH type of electron-phonon coupling holds significant promise for bipolaronic superconductivity because, for a single polaron,

the effective mass remains light even in the presence of Holstein-type electron-phonon coupling¹⁸ and with dispersive phonons¹⁹, which are more relevant to real materials. The light effective mass of the polaron in the strong electron-phonon coupling regime suggests the possibility of a light effective mass bipolaron, which could lead to the formation of a Bose-Einstein condensate-like superconductor in the low-density limit.

References^{12,13} investigate the Bose-Einstein condensation of bipolarons using the bond SSH model. In the absence of long-range Coulomb repulsion, this model has recently been shown to produce small-size, light-mass bipolarons that undergo a superfluid transition at high values of the critical transition temperature T_c ¹² in two dimensions. Reference¹³ demonstrates that even with the inclusion of long-range Coulomb repulsion, T_c remains significantly higher than that of Holstein bipolarons and can be on the order of, or greater than, the typical upper bounds for phonon-mediated T_c based on McMillan approximations in three dimensions. However, it raises the question of the extent to which the high T_c for bond bipolarons persists in two dimensions with long-range Coulomb interaction. Additionally, it is important to know the adiabatic regimes in which this high T_c could exist and the strength of the Coulomb interaction that can be tolerated while maintaining a high T_c . These considerations are crucial for understanding the potential of bond SSH bipolaron model as a mechanism for high-temperature superconductivity in low-dimensional systems for real materials.

In this paper, we investigate the effects of long-range Coulomb interaction on the superfluid transition temperature of the bond SSH bipolarons in two dimensions using a newly developed Quantum Monte Carlo method. Our approach is based on the path-integral formulation of the particle sector combined with real space diagrammatic techniques for the phonon sector²⁰. The results show that, in general, the long-range Coulomb interaction reduces T_c . Despite this reduction, T_c remains relatively high at $\omega/t = 1.0$ and 0.5 with $V = U/10$. The combination of light mass and relatively small size of bipolarons, even in the presence of long-range Coulomb repulsion,

accounts for the robustness of this mechanism and the relatively large values of T_c observed.

The rest of this paper is organized as follows. In Sec. II, we present the Hamiltonian of the bond SSH model. In Sec. III, we introduce the method and the properties measured for the bipolaron. In Sec. IV, we present the expression for the superfluid transition temperature of the bipolaron model. In Sec. V, we discuss the results, and Sec. VI concludes the paper.

II. HAMILTONIAN

We consider a bond SSH electron-phonon coupling on a simple two-dimensional square lattice. In this model, the electronic hopping between two sites is modulated by a single oscillator centered on the bond connecting the two sites. The model is described by the Hamiltonian^{21–24}:

$$\begin{aligned}
 H &= H_e + H_{ph} + H_{int} \\
 H_e &= -t \sum_{\langle ij \rangle, \sigma} (c_{j, \sigma}^\dagger c_{i, \sigma} + \text{H.c.}) + U \sum_i n_{i, \uparrow} n_{i, \downarrow} \\
 &\quad + \frac{1}{2} \sum_{i \neq j} V_{ij} n_i n_j \\
 H_{ph} &= \omega \sum_i (b_i^\dagger b_i + 1/2) \\
 H_{int} &= g \sum_{\langle ij \rangle, \sigma} (c_{j, \sigma}^\dagger c_{i, \sigma} + \text{H.c.}) X_{\langle ij \rangle} \\
 X_{\langle ij \rangle} &= b_{\langle ij \rangle}^\dagger + b_{\langle ij \rangle}
 \end{aligned} \tag{1}$$

with t the hopping amplitude of the electron. $\langle \dots \rangle$ denotes the nearest neighbor sites. $c_{i, \sigma}^\dagger$ ($c_{i, \sigma}$) is the electron creation (annihilation) operators on site i with spin $\sigma \in \{\uparrow, \downarrow\}$, and b_i^\dagger (b_i) is the phonon creation (annihilation) operators on site i . U is the on-site Hubbard repulsion and if not mentioned specifically, $U/t = 8.0$ is fixed. V is the nearest neighbor repulsion, and the long-range repulsive $V_{ij} = \frac{V_a}{|r_i - r_j|}$. $n_i = n_{i, \uparrow} + n_{i, \downarrow}$ and $n_{i, \sigma} = c_{i, \sigma}^\dagger c_{i, \sigma}$ at site i , and a is the lattice constant. ω is the phonon frequency and g is the electron-phonon coupling strength of the bond SSH type. $X_{\langle ij \rangle}$ is the oscillator associated with the bond connecting site i and j .

The properties of the bond SSH polaron is controlled by two parameters: (i) the effective coupling $\lambda = g^2/D/\omega$ with D the dimensionality of the system and $D = 2$, and (ii) the adiabaticity ratio ω/t . The most interesting regime in the adiabatic regime is $\omega/t \leq 1.0$, where the phonon degree of freedom is considered comparable or slow with respect to the electron motion. We analyze the model's behavior for two values of $\omega/t = 0.5$ and 1.0 . Both chosen values of ω/t are significantly smaller than the bare electronic bandwidth $W = 8t$ in 2D. Simulating values of ω/t smaller than 0.5 poses a computational challenge. In the following, we focus on results

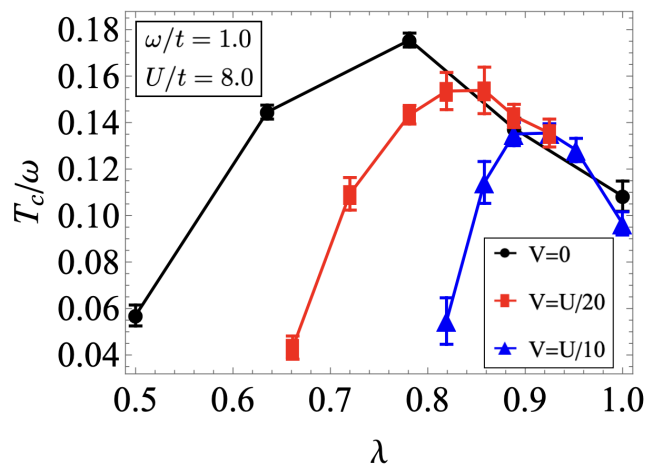


FIG. 1. Estimates of T_c/ω of the bond bipolaronic superconductor as a function of $\lambda = g^2/2/\omega$ for (a) different strengths of the Coulomb repulsion $V = 0$ (black dots), $V = U/20$ (red rectangles), and $V = U/10$ (blue up-triangles), at fixed phonon frequency $\omega/t = 1.0$ and on-site Hubbard repulsion $U/t = 8.0$, computed according to Eq. 2 from QMC simulations of the bipolaron effective mass m_{BP}^* and mean-square radius R_{BP}^2 . Error bars denote one standard deviation of statistical errors from the QMC simulations.

for $\omega/t = 0.5$ and 1.0 . Without specific explanation, we choose $U/t = 8.0$ based on the findings in Ref.¹², which demonstrates that T_c/ω exhibits a dome-like dependence on U/t . For a given electron-phonon coupling λ , T_c/ω peaks around the value of $U/t = 8.0$, which shows minimal variation with ω_0 in two dimensions. Additionally, $U/t = 8.0$ represents a regime where there is strong competition between the on-site Hubbard repulsion and the electronic kinetic energy.

III. METHOD

By employing a Quantum Monte Carlo (QMC) approach based on a path-integral formulation for the electronic sector and utilizing a real-space diagrammatic representation for the phonon sector²⁰, we investigate the singlet bipolaron formation in the two-electron sector of the model 1. The study of this specific bipolaron model is free from the sign problem, allowing us to achieve numerically exact results with minimal statistical errors on large lattices, even in the challenging regime where $\omega/t \leq 1.0$. We simulate the model on a two-dimensional square lattice with a linear size of $L = 140$ sites and open boundary conditions. This system size is sufficient to reach the thermodynamic limit and eliminate boundary effects.

In this paper, we measure the properties of the bipolaron like the binding energy, effective mass, and bipolaron size. *Binding energy*: the binding energy is defined as $\Delta_{\text{BP}}(\mathbf{k}) = 2E_{\text{p}}(\mathbf{k}) - E_{\text{BP}}(\mathbf{k})$ with $E_{\text{p}}(\mathbf{k})$ the single polaron energy. *Effective mass*: the bipolaron effective

mass is defined as $m_{\text{BP}}^* = \{[\partial E_{\text{BP}}(\mathbf{k})/\partial \mathbf{k}^2]|_{\mathbf{k}=0}\}^{-1}$ at momentum \mathbf{k} . *Mean-square radius*: the bipolaron mean-square radius is defined as $R_{\text{BP}}^2 = \langle \Psi_{\text{BP}} | \hat{R}^2 | \Psi_{\text{BP}} \rangle$ with Ψ_{BP} the bipolaron ground-state wave function.

IV. SUPERFLUID TRANSITION TEMPERATURE OF BIPOLARONS

A dilute system of electrons, at strong enough electron-phonon coupling, is unstable to the formation of bipolarons, leading to the formation of a gas of interacting bosons. These interacting bosons undergo a superfluid transition at the critical temperature T_c . Remarkably, when only the short-range/onsite interactions between bipolarons are considered, this temperature dependence exhibits a weak double-logarithmic relationship with the effective bipolaron-bipolaron interactions^{25–27}. In the presence of long-range Coulomb interaction, the value of T_c is reduced by around 15%²⁸. Hence, unless competing instabilities such as phase separation or Wigner crystallization are present (based on previous research, these instabilities are improbable), we can safely assume a 15% reduction in T_c when considering the Coulomb interaction between bipolarons.

With these considerations in mind, our focus shifts to analyzing the superfluidity of a gas comprising hardcore bipolarons with long-range Coulomb interactions in a two-dimensional lattice. Here, the critical temperature T_c is approximated by the expression $T_c \approx C \cdot 1.84 \cdot \frac{\rho_{\text{BP}}}{m_{\text{BP}}^*}$, where ρ_{BP} represents the density of bipolarons and m_{BP}^* denotes the effective mass of the bipolaron. The coefficient $C = 0.85$ accounts for the reduction in T_c due to the long-range Coulomb interaction between bipolarons²⁸. This formula holds true across a wide density range, provided that bipolarons do not overlap.

The maximum T_c achievable through this mechanism occurs when the density ρ_{BP} corresponds to a bosonic liquid with an interparticle spacing approximately equal to the radial size of the bipolaron R_{BP} , which, post lattice regularization, must be at least unity. Thus, ρ_{BP} can be estimated as $\min(1/(\pi R_{\text{BP}}^2), 1/\pi)$. From this, we derive an estimate for the maximum T_c of the Berezinskii-Kosterlitz-Thouless transition of the bipolaronic liquid, dependent solely on bipolaron properties by

$$T_c \approx \begin{cases} \frac{0.5}{m_{\text{BP}}^2 R_{\text{BP}}^2} & \text{if } R_{\text{BP}}^2 \geq 1, \\ \frac{0.5}{m_{\text{BP}}^2} & \text{otherwise.} \end{cases} \quad (2)$$

We henceforth refer to this optimized T_c simply as T_c in subsequent discussions and figures. In summary, bipolarons experience a superfluid transition at a temperature determined by the properties of the single bipolaron, as bipolaron size and effective mass.

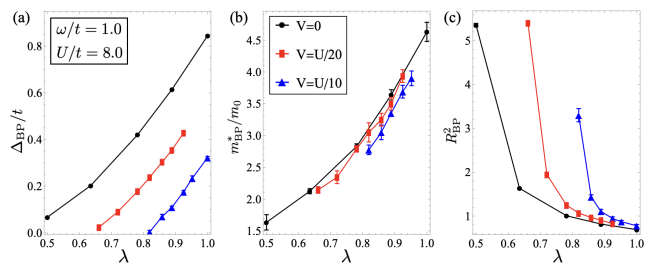


FIG. 2. Bipolaron properties computed from QMC calculations performed on Eq. 1 at adiabaticity parameter $\omega/t = 1.0$ as a function of the electron-phonon coupling λ for on-site Hubbard repulsion $U/t = 8.0$ with different Coulomb interactions $V = 0$, $V = U/20$, and $V = U/10$. (a) Bipolaron binding energy Δ_{BP} in units of the electron hopping t . (b) Bipolaron effective mass m_{BP}^* in units of the mass of two free electrons $m_0 = 2m_e = 1/t$. (c) Bipolaron mean-square radius R_{BP}^2 . Error bars denote one standard deviation of statistical errors from the QMC simulations.

V. RESULTS AND DISCUSSION

Figure 1 shows the superfluid transition temperature, denoted as T_c/ω in units of the phonon frequency ω , for the bond bipolaron as a function of $\lambda = g^2/2/\omega$ at phonon frequency $\omega/t = 1.0$ and an on-site Hubbard repulsion $U/t = 8.0$, with various Coulomb interactions $V = 0$, $U/20$, and $U/10$. The reentrant behavior of the optimal T_c (an initial increase followed by a decrease in T_c with increasing λ) is clearly shown in Fig. 1, as observed in Ref. 12,13. The interaction V/U was chosen to be $1/10$ as this is a reasonable estimate for many materials¹³. In Figure 1, the optimal T_c for $V/U = 1/20$ (red rectangles) decreases by only about 7% compared to the case without Coulomb interaction (black dots). With $V/U = 1/10$, which represents a relatively large Coulomb interaction, the optimal T_c is reduced by around 20%. Therefore, the findings in Fig. 1 demonstrate that bipolaronic superconductivity remains robust even under strong, poorly screened Coulomb repulsion. The values of T_c do not decrease significantly at optimized electron-phonon coupling strength λ , despite the presence of strong Coulomb repulsion. This is significant because in many other models, like the Holstein model, strong Coulomb repulsion typically lowers T_c . However, in the bond model, the bipolarons manage to maintain high T_c values even when $V = U/10$.

Figure 2 presents the features of bipolarons, specifically binding energy (a), bipolaron effective mass (b), and bipolaron mean-square radius (c), in the presence of long-range Coulomb repulsion with values $V = 0$, $U/20$, and $U/10$. From the binding energy required to form a bipolaron, as shown in Fig. 2(a), it is evident that the coupling strength needed to form a bipolaron increases with the Coulomb interaction. This indicates that stronger electron-phonon coupling is necessary to overcome the repulsive Coulomb forces to form a stable bipo-

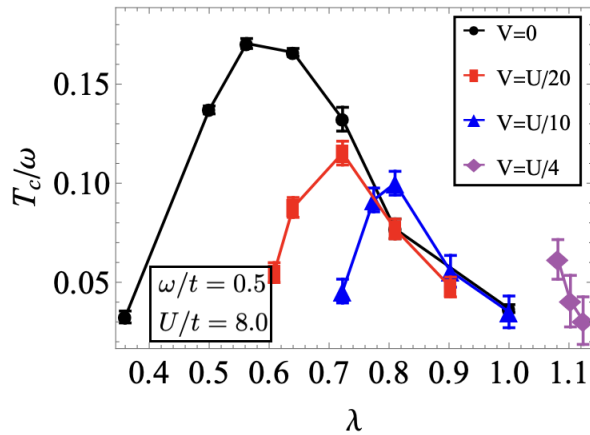


FIG. 3. Estimates of T_c of the bond SSH bipolaronic superconductor as a function of $\lambda = g^2/2/\omega$ for (a) different strengths of the Coulomb repulsion $V = 0$ (black dots), $U/10$ (red rectangles) and $U/20$ (blue up-triangles) at fixed on-site interaction $U/t = 8.0$, computed according to Eq. 2 from QMC simulations of the bipolaron effective mass m_{BP}^* and mean-square radius R_{BP}^2 . Error bars denote one standard deviation of statistical errors from the QMC simulations.

laron. Furthermore, Fig.2(b) demonstrates that at the same coupling strength, the effective mass of the bipolaron decreases as the Coulomb repulsion V increases. This decrease in effective mass suggests that the bipolaron becomes lighter with stronger Coulomb repulsion at the same coupling strength λ . Conversely, the size of the bipolaron, depicted in Fig.2(c), increases as V increases at the same coupling strength λ , indicating that the spatial extent of the bipolaron expands under stronger Coulomb interaction. Figs. 2(b) and (c) show that small-size bipolarons with $R_{\text{BP}} < 1.5$ exhibit rather weak effective mass enhancement $m_{\text{BP}}^* < 4.0$. The changes in the effective mass and bipolaron size are relatively mild, resulting in changes in the optimal superfluid transition temperature T_c of less than 20%.

Figure 3 illustrates the superfluid transition temperature, denoted as T_c/ω , for the bond bipolaron as a function of $\lambda = g^2/2/\omega$ with $\omega/t = 0.5$, $U/t = 8.0$, and various Coulomb interactions $V = 0$, $U/20$, $U/10$, and $U/4$. Even with $V = U/10$, the optimal T_c remains relatively high compared to the case without Coulomb interaction (depicted by black dots). The values of T_c/ω for the bond bipolarons appear to be comparable to or greater than the upper bound of 0.05 predicted by McMillan's phenomenological approach to Migdal-Eliashberg theory in the adiabatic limit for moderate values of $\lambda \lesssim 1$. McMillan's formula $\frac{T_c}{\omega} = \frac{1}{1.45} \exp\left(-1.04 \frac{1+\lambda}{\lambda - \mu^* (1+0.62\lambda)}\right)$, where $\mu^* = 0.12$ represents the Coulomb pseudo-potential commonly found in many materials, predicts an upper bound of $T_c/\omega \sim 0.05$ at $\lambda = 1$. In other words, our calculation predicts T_c values higher than typical experimental findings in dilute superconductors. Notably, as V increases to $U/4$, there is no reentrance of T_c , and the value is less

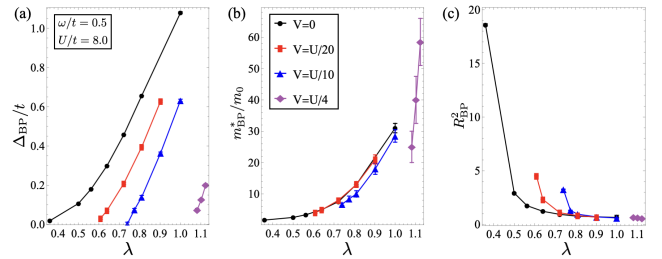


FIG. 4. Bipolaron properties in the bond model. Bipolaron properties computed from QMC calculations performed on Eq. 1 at adiabaticity parameter $\omega/t = 1.0$ as a function of the electron-phonon coupling λ for different on-site Hubbard $U/t = 8.0$ with Coulomb interaction $V = 0$, $V = U/10$, and $V = U/20$. (a) Bipolaron binding energy Δ_{BP} in units of the electron hopping t . (b) Bipolaron effective mass m in units of the mass of two free electrons $m_0 = 2m_e = 1/t$ (c) its mean-squared radius R^2 . Error bars denote one standard deviation of statistical errors from the QMC simulations.

than 0.05. This is because, at such a large Coulomb interaction, the bipolaron forms a strongly bound state. Once formed, the effective mass increases abruptly, and the bipolaron size is confined within one lattice space since the two electrons are tightly bound together, as shown in Fig. 4. Consequently, T_c is ultimately suppressed by Coulomb interaction at $\omega/t = 0.5$ with Coulomb interaction $V = U/4$.

Figure 5 shows the superfluid transition temperature T_c/ω for different values of $U/t = 6.0$ and 8.0 , with $V = U/10$ and $\omega/t = 0.5$. The optimal T_c stays the same within the margin of error across these two different values of U/t .

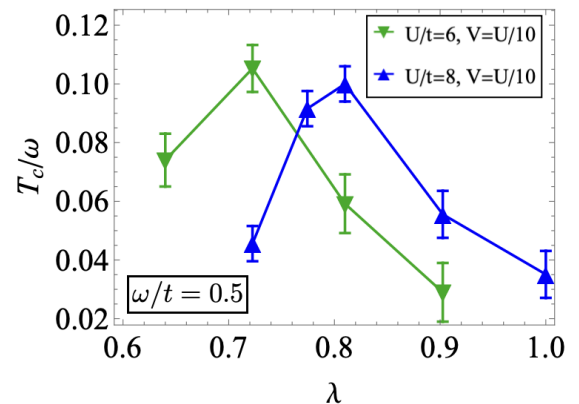


FIG. 5. Estimates of T_c/ω of the bond bipolaronic superconductor as a function of $\lambda = g^2/2/\omega$ for different strengths of the on-site interaction U at fixed $V = U/10$. Error bars denote one standard deviation of statistical errors from the QMC simulations.

VI. CONCLUSION

As a summary, we investigate the superfluid transition temperature of the bond bipolarons in a 2D square lattice. The results show that in general the long-range Coulomb interaction reduces T_c . Despite this reduction, T_c remains relatively high at $\omega/t = 1.0$ and 0.5 with $V = U/10$. The combination of light mass and relatively small size of bipolarons, even in the presence of long-range Coulomb repulsion, accounts for the robustness of this mechanism and the relatively large values

of T_c observed. This study shows a feature with significant implications for understanding and manipulating electron-phonon interactions in advanced materials and quantum systems.

ACKNOWLEDGMENTS

This work is supported by the National Natural Science Foundation of China (NSFC) under Grants No. 12204173 and 12275002, and the University Annual Scientific Research Plan of Anhui Province under Grant No. 2022AH010013.

-
- * chaozhang@ahnu.edu.cn
- ¹ L. D. Landau, *Z. Sowjetunion* **3**, 664 (1933).
 - ² H. Fröhlich, H. Pelzer, and S. Zienau, *Philos. Mag.* **41**, 221 (1950).
 - ³ R. P. Feynman, *Phys. Rev.* **97**, 660 (1955).
 - ⁴ T. D. Schultz, *Phys. Rev.* **116**, 526 (1959).
 - ⁵ T. Holstein, *Ann. Phys.* **8**, 325 (1959).
 - ⁶ A. S. Alexandrov and P. E. Kornilovitch, *Phys. Rev. Lett.* **82**, 807 (1999).
 - ⁷ T. Holstein, *Ann. Phys.* **281**, 725 (2000).
 - ⁸ B. K. Chakraverty, J. Ranninger, and D. Feinberg, *Phys. Rev. Lett.* **81**, 433 (1998).
 - ⁹ J. Bonča, T. Kataršnik, and S. A. Trugman, *Phys. Rev. Lett.* **84**, 3153 (2000).
 - ¹⁰ A. Macridin, G. A. Sawatzky, and M. Jarrell, *Phys. Rev. B* **69**, 245111 (2004).
 - ¹¹ N. Prodanović and N. Vukmirović, *Phys. Rev. B* **99**, 104304 (2019).
 - ¹² C. Zhang, J. Sous, D. R. Reichman, M. Berciu, A. J. Millis, N. V. Prokof'ev, and B. V. Svistunov, *Phys. Rev. X* **13**, 011010 (2023).
 - ¹³ J. Sous, C. Zhang, M. Berciu, D. R. Reichman, B. V. Svistunov, N. V. Prokof'ev, and A. J. Millis, *Phys. Rev. B* **108**, L220502 (2023).
 - ¹⁴ P. E. Kornilovitch and E. R. Pike, *Phys. Rev. B* **55**, R8634 (1997).
 - ¹⁵ D. J. J. Marchand, G. De Filippis, V. Cataudella, M. Berciu, N. Nagaosa, N. V. Prokof'ev, A. S. Mishchenko, and P. C. E. Stamp, *Phys. Rev. Lett.* **105**, 266605 (2010).
 - ¹⁶ C. Zhang, N. V. Prokof'ev, and B. V. Svistunov, *Phys. Rev. B* **104**, 035143 (2021).
 - ¹⁷ M. R. Carbone, A. J. Millis, D. R. Reichman, and J. Sous, *Phys. Rev. B* **104**, L140307 (2021).
 - ¹⁸ C. Zhang, *Phys. Rev. B* **109**, 165119 (2024).
 - ¹⁹ C. Zhang, *Phys. Rev. B* **108**, 075156 (2023).
 - ²⁰ C. Zhang, N. V. Prokof'ev, and B. V. Svistunov, *Phys. Rev. B* **105**, L020501 (2022).
 - ²¹ W. P. Su, J. R. Schrieffer, and A. J. Heeger, *Phys. Rev. Lett.* **42**, 1698 (1979).
 - ²² S. Barišić, J. Labbé, and J. Friedel, *Phys. Rev. Lett.* **25**, 919 (1970).
 - ²³ S. Barišić, *Phys. Rev. B* **5**, 932 (1972).
 - ²⁴ S. Barišić, *Phys. Rev. B* **5**, 941 (1972).
 - ²⁵ D. S. Fisher and P. C. Hohenberg, *Phys. Rev. B* **37**, 4936 (1988).
 - ²⁶ N. Prokof'ev, O. Ruebenacker, and B. Svistunov, *Phys. Rev. Lett.* **87**, 270402 (2001).
 - ²⁷ S. Pilati, S. Giorgini, and N. Prokof'ev, *Phys. Rev. Lett.* **100**, 140405 (2008).
 - ²⁸ C. Zhang, B. Capogrosso-Sansone, M. Boninsegni, N. V. Prokof'ev, and B. V. Svistunov, *Phys. Rev. Lett.* **130**, 236001 (2023).